# Mobility in UTB-SOI PFETS: Local Coordinate-Based Modeling with the Density Gradient Method

Daniel Connelly (djconnel@ieee.org), D.E. Grupp : Acorn Technologies, Palo Alto, CA;

Paco Leon, Dan Yergeau : Mixed Technology Associates, Palo Alto, CA

***Abstract*—Here, for the first time, a local coordinate-based method is used to model surface acoustic phonon and thickness variation scattering in $Si/SiO_2$ PMOS structures using the density-gradient method. A reduction in mobility below that predicted by the electric-field based "universal mobility" curves for ultra-thin-body SOI devices is predicted in excellent agreement with recently published experimental data. An extension to multiple dimensions, demonstrated with some simple examples, is then applied to cylindrical devices, showing the mobility reduction of two-dimensional confinement.**

## I. Introduction

CARRIERS in a MOS inversion layer are subject to scattering associated both with the $Si/SiO_2$ interface and with confinement against the interface. Takagi [1] [2] described this in terms of the "effective electric field" ($E_{eff}$), slightly modified by [3]:

$$E_{eff} = (q/\epsilon_{Si})\,(\langle N_{dpl}\rangle + \eta N_s)\ , \qquad (1)$$

where $\epsilon_{Si}$ is the permittivity of Si, $q$ is the charge quantum, $\langle N_{dpl}\rangle$ is the average sheet density of ionized impurities under[1] inversion layer carriers, $N_s$ is the inversion charge area density, and $\eta$ for holes on (001) Si is 1/3. This works in bulk devices where the potential well is due to the surface electric field, but in ultra-thin-body (UTB) SOI structures, there is a potential well even without an electric field. Thus, the $E_{eff}$ approach is inadequate where structural confinement from multiple interfaces is significant. A simple, computationally efficient, local approach to mobility modeling, which matches both the case of electric field and structural confinement, is highly desirable. Here, for the first time, a coordinate-based approach to modeling mobility components for holes is presented. It is loosely based on a one-dimensional (1-d) effective mobility relationship presented in [4], but is applied locally, and an extension from one to three dimensions is proposed.

## II. Density Gradient Method

Coordinate-based mobility modeling, and electrostatic modeling of UTB SOI structures, requires a suitable prediction of the true hole distribution. The density gradient (DG) method [5] fills this need in a relatively computationally efficient fashion applicable to one, two, or three dimensions. DG parameters used here include $m_e^* = 0.26$ and $m_h^* = 0.16$. 1-d results, generated with *Prophet*[11], compare favorably with *Schred* data (Fig. 1 and 2).

## III. Mobility Modeling

### A. Overview

Mobility modeling was based on the approach of Agostinelli *et al* [6]. The three scattering mechanisms of

[1] "Under" in this context means further from the appropriate $Si/SiO_2$ interface.

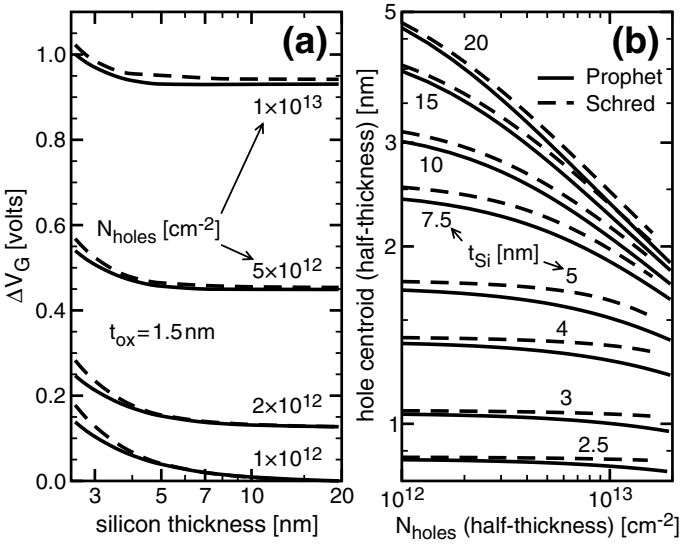


Fig. 1. Parametric comparison of ultra-thin-body symmetric dual-gate Si structures simulated with *Schred* or *Prophet*, the latter using the density gradient method. (a) Gate voltage needed to reach given hole density integrated over the Si half-thickness, relative to $10^{12}/\mathrm{cm}^2$ for thick Si. (b) Centroid of hole density in the Si half-thickness.

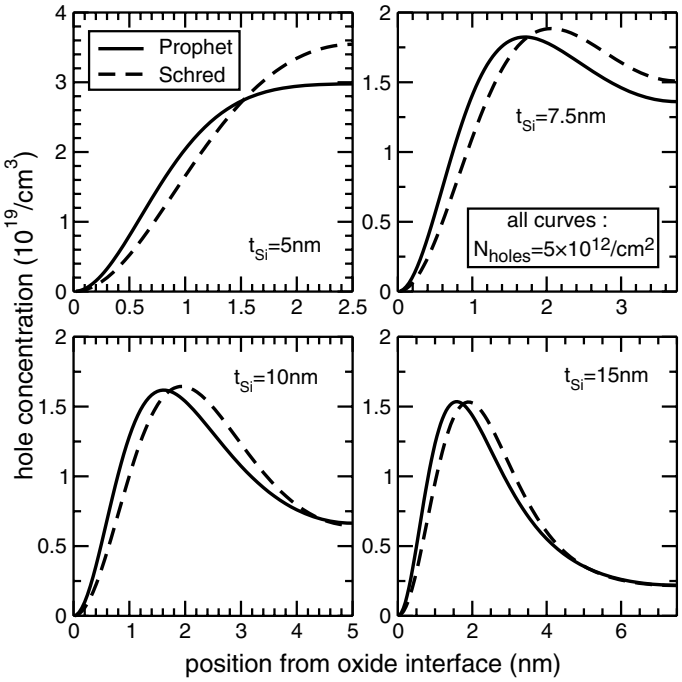


Fig. 2. Comparison of hole profiles in ultra-thin-body symmetric dual-gate Si structures of various thicknesses, as predicted by *Schred*, or *Prophet* with the density gradient method, for $5\times10^{12}/\mathrm{cm}^2$ holes in the Si half-thickness.


0-7803-7826-1/03/$17.00 © 2003 IEEE

that work were used here: coulombic scattering, acoustic phonon scattering, and surface roughness scattering. A fourth scattering mechanism, described by Uchida *et al* [7], occurs in regions of electron confinement. If the confining dimension is position-dependent, the local ground-state energy becomes position-dependent, exposing moving electrons to a time-dependent potential. The resulting scattering is further addressed in Section III-C. These four mobility components were combined, following the practice of [6], using Mathiessen's rule.[2]

Coulombic scattering was handled with an Agostinelli *et al* variant described in [9], which depends on local hole concentration, rather than the original form in [6], which uses $E_{eff}$.

Surface scattering was modeled using the $\mu_{eff}$ *vs.* $E_{eff}$ surface scattering relationship of Agostinelli *et al* applied equally to all holes in a one-dimensional slice. $E_{eff}$ was calculated at the channel surface via (1). The model could be fully localized by using a local surface scattering model such as that of Darwish *et al* [10].[3] Extension of surface scattering modeling to include the effect of structural confinement is an opportunity for advancement of this work.

Acoustic phonon scattering was localized using a coordinate-based approach, as described next.

### B. Acoustic Phonon Scattering

The key to this method is the parameter $\gamma$:

$$\text{1-d} \quad : \quad \gamma^2 = \frac{1}{r_+^2} + \frac{1}{r_-^2}\,, \tag{2}$$

$$\text{2-d} \quad : \quad \gamma^2 = \frac{2}{\pi}\int_0^{2\pi} \frac{d\theta}{r_\theta^2}\,, \tag{3}$$

$$\text{3-d} \quad : \quad \gamma^2 = \frac{3}{2\pi}\iint \frac{d^2\mathbf{\Omega}}{r_{\mathbf{\Omega}}^2}\,. \tag{4}$$

In (2), $r_\pm$ is the distance to the nearest $SiO_2$ interface in the positive (+) or negative (−) direction. In (3), $r_\theta$ is the distance to the nearest $Si/SiO_2$ interface in direction $\theta$, with the integral over the unit circle. In (4), the integral is over the unit sphere, where $d^2\mathbf{\Omega}$ is the differential solid angle, and $r_{\mathbf{\Omega}}$ is the distance to the nearest $Si/SiO_2$ interface in direction $\mathbf{\Omega}$. The fixed coefficients in these equations were derived to yield the same $\gamma$ in the case of a planar interface.

In the quantum limit for a single $Si/SiO_2$ interface, the inversion layer width is inversely proportional to the one-third power of the effective field [2]. Thus, assuming $\langle 1/\gamma \rangle$, which in the single-interface case is proportional to the mean distance to the interface, is roughly proportional to the inversion width, $E_\gamma$, a substitute for $E_{eff}$, is defined:

$$\frac{\epsilon_{Si} E_\gamma}{q} \equiv N_\gamma = (k_\gamma \gamma)^3\ . \tag{5}$$

Here $k_\gamma$ a fitting term for which $25.1\,\mu\text{m}^{1/3}$ was found to match the bulk data well. $E_\gamma$ of (5) is substituted locally for $E_{eff}$ in the $\mu_{eff}$ *vs.* $E_{eff}$ acoustic phonon scattering (APS) formula of Agostinelli *et al* [6] to yield a local quantity; the "effective mobility" relationship is thus directly localized. The $\gamma$ field thus depends only on the physical structure, and need not be recalculated during bias change or solution iteration.

### C. Thickness Variation Scattering

As was previously noted, [7] shows that for thin Si films, local variation in Si thickness ($\sigma_t$) results in a modulation of local ground state energy, yielding an effective scattering potential. This scattering is proportional to $1/t_{Si}^6$. However, for this to be useful, it needs to be extended to multiple dimensions.

A way of doing this in continuous fashion, consistent with the one-dimensional form, is to follow an analogous approach to that used for acoustic phonon scattering. A local parameter, $\gamma_t$, is defined:

$$\text{1-d} \quad : \quad \gamma_t^6 = \frac{1}{(r_+ + r_-)^6}\,, \tag{6}$$

$$\text{2-d} \quad : \quad \gamma_t^6 = \frac{16}{5\pi}\int_0^{\pi} \frac{d\theta}{(r_\theta + r_{\pi+\theta})^6}\,, \tag{7}$$

$$\text{3-d} \quad : \quad \gamma_t^6 = \frac{7}{2\pi}\iint \frac{d^2\mathbf{\Omega}}{(r_{\mathbf{\Omega}} + r_{-\mathbf{\Omega}})^6}\,, \tag{8}$$

where the integral in (8) is over the half-sphere. The scattering is proportional to $\gamma_t^6$. This approach is equivalent to thinking of a point in space as surrounded by an array of differentially-sized cavities, with each contributing to scattering in proportion to its angle or solid angle subtended. Calibration to the data from [7] yielded an associated mobility component $\mu_{\sigma t} = (1.36\,\text{nm}\,\gamma_t)^{-6}\ \text{cm}^2/\text{V-sec}$, although the coefficient is expected to depend on the thickness variation characteristics of a particular process and material.

## IV. One-Dimensional Results

Simulations were done with *Prophet* at $T = 300\,\text{K}$ unless specified, with mobility post-processed.

Some results are plotted in Fig. 3: (a) The local $\gamma$-based approach and the nonlocal $E_{eff}$-based [6] calculations of APS yield essentially fully overlapping curves for 300 K bulk devices. (b) The bulk mobility temperature dependence is also a good match. (c-d) Measured data from [4] compares favorably to modeled data with the simple interface charge model from [6].

A comparison to the more aggressively scaled data from [7] is shown in Fig. 4. Below 5 nm, mobility in the actual devices falls more sharply than is predicted without including $\sigma_t$ scattering. The calibrated $\mu_{\sigma t}$ model (6) improves the fit in this region.

## V. Two-Dimensional Results

### A. Acoustic Phonon Scattering

Two-dimensional calculations of acoustic phonon scattering can be done using (3). A sample result, showing $\gamma$ in the vicinity of convex and concave corners, is plotted in Fig. 5. There is a small anomaly when $x = 0$ or

[2] See, for example, Section 4.3.2 of [8].

[3] The Darwish *et al* model was not used here due to its artificial doping dependence.


0-7803-7826-1/03/$17.00 © 2003 IEEE

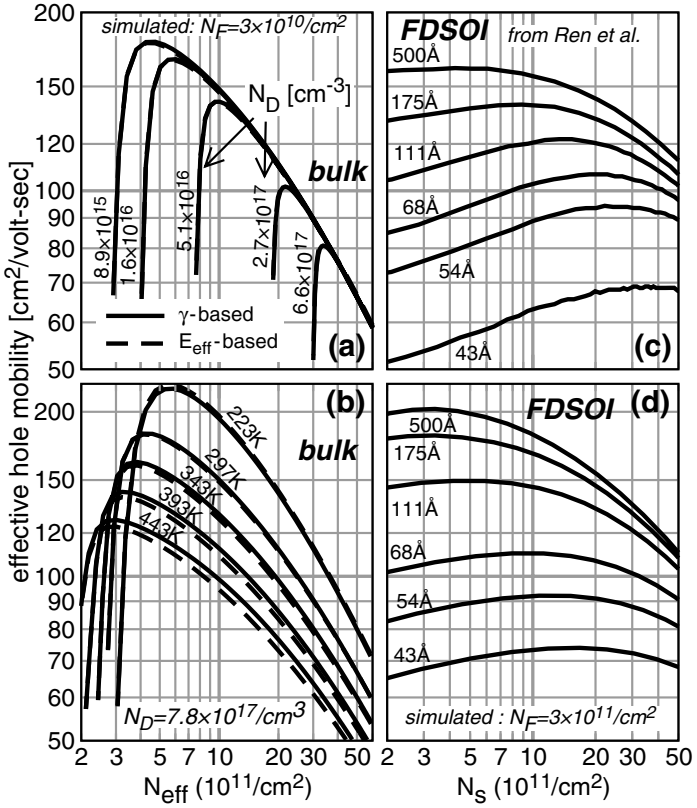


Fig. 3. (a) Comparison of bulk mobility modeled using either a direct calculation of effective field, or the $\gamma$-based approach using (5) with $k_\gamma = 25.1\,\mu\mathrm{m}^{1/3}$. The curves essentially fully overlap. (b) The effect of temperature on the bulk mobility fit. (c) Measured data from [4]. (d) $\gamma$-based model of same devices, using $N_F = 3{\times}10^{11}/\mathrm{cm}^2$.

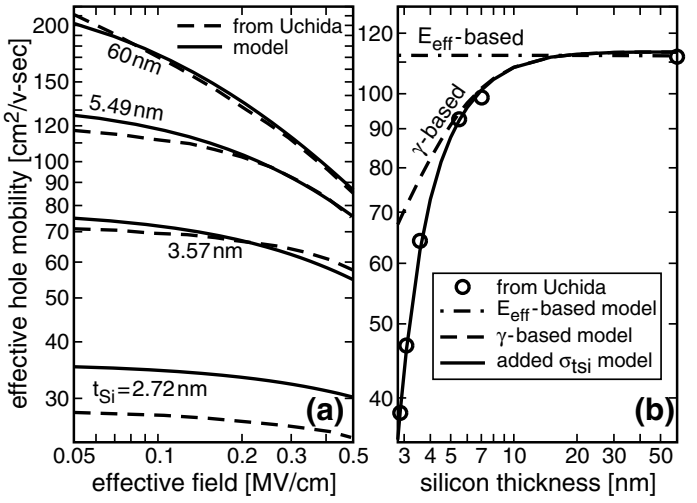


Fig. 4. (a) Comparison of $\mu_{eff}$-*vs.*-$E_{eff}$ curves for UTB PFETs from [7]. Simulations assumed $N_F = 0$. (b) Interpolated mobility at $E_{eff} = 0.3\,\mathrm{MV/cm}$, or $N_{eff} = 1.94{\times}10^{12}/\mathrm{cm}^2$. The $\gamma$ model matches results well from middle-$t_{Si}$ range, while the $E_{eff}$ model fails to predict significant $t_{Si}$ dependence. At low-$t_{Si}$, the $1/t_{Si}^6$-proportional thickness variation ($\sigma_t$) scattering term becomes important.

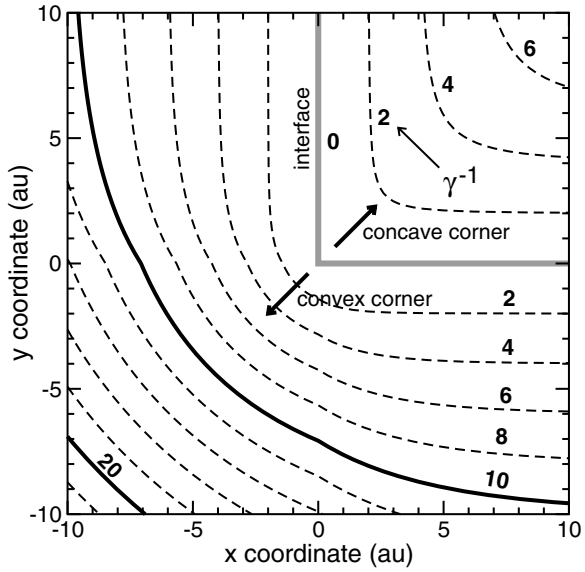


Fig. 5. 2-d calculation of $1/\gamma$ in the vicinity of convex and concave corners. In each region (upper right, remainder), assume the opposite region is $SiO_2$.

$y = 0$ is crossed and sides become occluded, demonstrating a simplification of the model. In the surface-APS-limited regime, mobility is roughly proportional to $1/\gamma$, and thus this is essentially a plot of this mobility component.

### *B. Thickness Variation Scattering*

An example of the $\sigma_t$ scattering described by (7) is shown in Fig. 6(a). In the semi-infinite region there is no structural confinement, and thus there is no $\sigma_t$ scattering. As the thin Si region is penetrated, however, the scattering quickly yet continuously approaches the 1-d limit.

Fig. 6(b) shows a corner of a Si box. Plotted here is the inverse of the prior plot – contours proportional to $\mu_{\sigma t}$. Points in the corners are within the close proximity of the two adjacent sides, which yield a large sensitivity to interfacial roughness.

## VI. Application : Gate Design Comparison

In this section, the predictions of the simple $\gamma$-based model on the effect of gate design on effective hole mobility is examined. Three designs were considered, each with Si regions doped $10^{14}/\mathrm{cm}^3$ $n$-type:

1. A single-gate structure, with a 400 nm buried oxide.
2. A dual-gate structure.
3. A cylindrical structure, with body diameter $t_{Si}$.

All carrier profiles were generated in one dimension. Cylindrical coordinates were used for the cylindrical device. Charge integrals were normalized to net "channel" area, the area of the Si surface in contact with gate oxide. The $\sigma_t$ term was omitted.

The $\gamma$ field is the same for the single-gate and dual-gate structures, but in the center of the cylindrical structure it is a factor $\sqrt{2}$ larger. This results in a comparable reduction in effective mobility as the carriers are squeezed into this region, as seen in Fig. 7. Smaller mobility is as ex-


0-7803-7826-1/03/$17.00 © 2003 IEEE

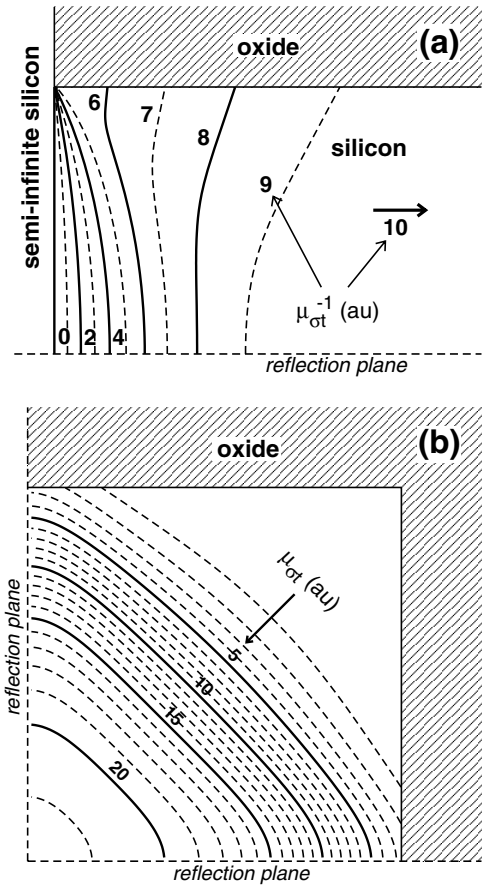


Fig. 6. 2-d $\sigma_t$ scattering-limited mobility ($\mu_{\sigma t}$) examples. In each case $\mu_{\sigma t}$ is proportional to the sixth power of the dimensional scale, which is unspecified. (a) $1/\mu_{\sigma t}$ contours of thin film in contact with a semi-infinite Si region. (b) Contours proportional to $\mu_{\sigma t}$ in a Si square region, of which a quarter is shown.

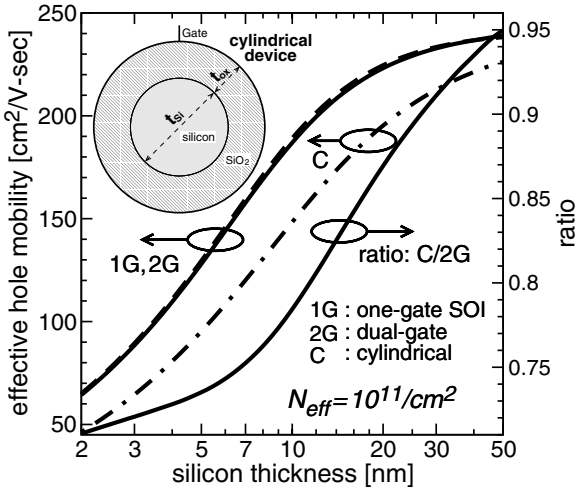


Fig. 7. Mobility in an APS limited regime for three structures. The mobility is suppressed in the cylindrical structure due to the additional confinement dimension. The dual-gate structure has essentially the same mobility as the single-gate SOI, despite the somewhat different carrier distributions in the middle-thickness region. The mobility reduction in the cylindrical device approaches, for small $t_{Si}$, the $\gamma$-ratio limit of $\sqrt{1/2}$ as the hole density peak moves to the Si center. Oxide thickness $t_{ox}$ isn't relevant to this plot.

pected due to the additional dimension of confinement in the cylindrical case.

If $\sigma_t$ scattering is applied to the comparison of dual-gate to cylindrical devices, the mid-body mobility ratio in the small-geometry limit becomes greater: 6.4 via Equation 7, substantially more than the APS-limited ratio of $\sqrt{2}$.

## VII. Conclusion

A simple coordinate-based approach, applied to results of the density gradient model, is able to localize the effective-field-based mobility relationships in the APS-limited regime of bulk PFETs. This method closely matches behavior seen in published experimental thin-film data for films at least 5 nm thick. Below 5 nm, thickness variation ($\sigma_t$) scattering becomes important. An extension to two and three dimensions of both APS and thickness variation scattering was demonstrated with some simple test cases. An application of the model to cylindrical and UTB MOSFETs predicts a reduction in APS-limited mobility by up to a factor $\sqrt{2}$, and $\sigma_t$-limited mobility by up to a factor 6.4, when structural confinement extends from one to two dimensions.

## References


[1] S. Takagi, A. Toriumi, M. Iwase, and H. Tango, "On the universality of inversion layer mobility in Si MOSFETs: part I – effects of substrate impurity concentration," *IEEE Trans. on Electron Devices*, vol. 41, no. 12, pp. 2357–2362, Dec 1994.

[2] S. Takagi, A. Toriumi, M. Iwase, and H. Tango, "On the universality of inversion layer mobility in Si MOSFETs: part II – effects of surface orientation," *IEEE Trans. on Electron Devices*, vol. 41, no. 12, pp. 2363–2368, Dec 1994.

[3] D. Vasileska, P. Bordone, T. Eldridge, and D.K D.K. Ferry, "Quantum transport calculations for silicon inversion layers in MOS structures," *Physica B*, vol. 227, no. 1-4, pp. 333–5, Sep 1996.

[4] Z. Ren, S. Hegde, B. Doris, P. Oldiges, T. Kanarsky, O. Dokumaci, R. Roy M. Ieong, E.C. Jones, and H.-S.P. Wong, "An experimental study on transport issues and electrostatics of ultrathin body SOI pMOSFETs," *IEEE Electron Device Lett.*, vol. 23, no. 10, pp. 609–611, Oct 2002.

[5] M.G. Ancona and G.J. Iafrate, "Quantum correction to the equation of state of an electron gas in a semiconductor," *Physical Review B*, vol. 39, no. 13, pp. 9536, 1989.

[6] V.M. Agostinelli, H. Shin, and A.F. Tasch, "A comprehensive model for inversion layer hole mobility for simulation for submicrometer MOSFETs," *IEEE Trans. on Electron Devices*, vol. 38, pp. 151–159, Jan 1991.

[7] K. Uchida, H.Watanabe, A. Kinoshita, J. Koga, T.Numata, and S. Takagi, "Experimental study on carrier transport mechanism in ultrathin-body SOI n- and p- MOSFETs with SOI thickness less than 5 nm," in *2002 IEEE IEDM Tech. Digest*, 2002, pp. 47–50.

[8] M. Lundstrom, *Modular Series of Semiconductor Devices Volume X: Fundamentals of Carrier Transport*, Addison-Wesley, 1990.

[9] Avanti Corporation TCAD Business Unit, Fremont, CA, *Medici : Two Dimensional Device Simulation Program User's Manual*, 2000.2 edition, Jul 2000.

[10] M. N. Darwish, J. L. Lentz, M. R. Pinto, P. M. Zeitzoff, T. Krutsick, and H. H. Vuong, "An improved electron and hole mobility model for general purpose device simulation," *IEEE Trans. on Electron Devices*, vol. 44, no. 9, pp. 1529–1538, Sep 1997.

[11] C.S Rafferty, Z. Yu, B. Biegel, M.G. Ancona, J. Bude, and R.W. Dutton, "Multi-dimensional quantum effect simulation using a density-gradient model and script-level programming techniques," in *1998 IEEE SISPAD Proc.*, 1998, pp. 137–140.